

Probabilistic Hierarchical Spatial Model for Mine Locations and its Application in Robotic Landmine Search

Yangang Zhang, Mark Schervish, Howie Choset

Carnegie Mellon University, Pittsburgh, USA. *yazhang,mark,choset+@andrew.cmu.edu*

Abstract

One way to improve the efficiency of mine search, compared with a complete coverage algorithm, is to direct the search based on the spatial pattern of the minefield. This paper extends our original statistical approach [9] to identify the regular pattern of a minefield at the beginning of the searching process. The extracted pattern parameters are used to build a probability distribution map of the configuration of the minefield. The map then can be used to guide the search for more mines efficiently. The new approach can efficiently capture the systematic and accumulated random departure of the actual mine locations from the grid pattern caused by the inaccuracy of the translational and rotational motion of the mine layer. Online implementation of our approach on a mobile robot is feasible.

1 Introduction

The problem of detecting and cleaning surface-laid mines using mobile robots is of great interest to civilians and military alike. One critical step of de-mining is to pass the mine detector to cover the minefield to locate the mines. An exhaustive coverage algorithm [2, 3] is a path planning technique where the robot explicitly passes over all points in the minefield at least once. Exhaustive coverage is the best strategy when the robot has unlimited time and a perfect mine detector.

However, in many situations time or power limitation may not permit covering a target environment completely. Probabilistic path planning technology can significantly extend the capabilities of current sensors in such de-mining applications. Probabilistic path planning utilizes a probability density map of the mine locations to opportunistically guide an agent to locate mines to increase the number of the found mines within the time and resource limitation compared to completed coverage. For example, a robot equipped with a probabilistic path planner will search first the area which has higher probability to have mines, then move to the lower probability area.

The work of [5] provides a more detailed discussion of a probabilistic path planning algorithm given a known probability density map. In most of the situations, the probability density map is unknown, in which, the map has to be built before the path planning begins. Being able to build a map quickly and accurately by analyzing the sensor information collected by the robot searching a small sample area of the minefield is critical for successfully applying the probabilistic path planning.

In this paper, we extend our original statistical method [9] to efficiently build a probability density map of mine locations when mines are intended to be laid in a regular pattern. The new approach can efficiently capture the systematic and accumulated random departure of the actual mine locations from the intended pattern caused by the inaccuracy of the translational and rotational motion of the mine layer.

Following our previous work [9], we assume that the intended minefield pattern is a regular row-shifted grid pattern (See Figure 1(a) for the intended pattern and Figure 1(b) for the actual laid mine positions.), which is commonly used in mine deployment operation [1]. Our strategy is to search a small sample area A of a minefield and then to recognize the underlying intended pattern which best matches the found mine locations in A as shown in Figure 1(c). Finally, a probability density map of the mine locations is constructed based on the recognized pattern. In this paper, we focus on presenting the pattern recognition algorithm which is a generalization of our previous work [9].

In Section 2 and 3, we build the link between the new recognition method and the prior work [9]. Section 4 describes a hierarchical probability model to specify probability law of the difference between the detected mine locations and the intended pattern. The probability model is used to construct a likelihood function, which provides a matching function between the detected mine locations and the intended pattern. Derivation of the likelihood function is shown in section 5. A Maximum Likelihood Estimator (MLE)

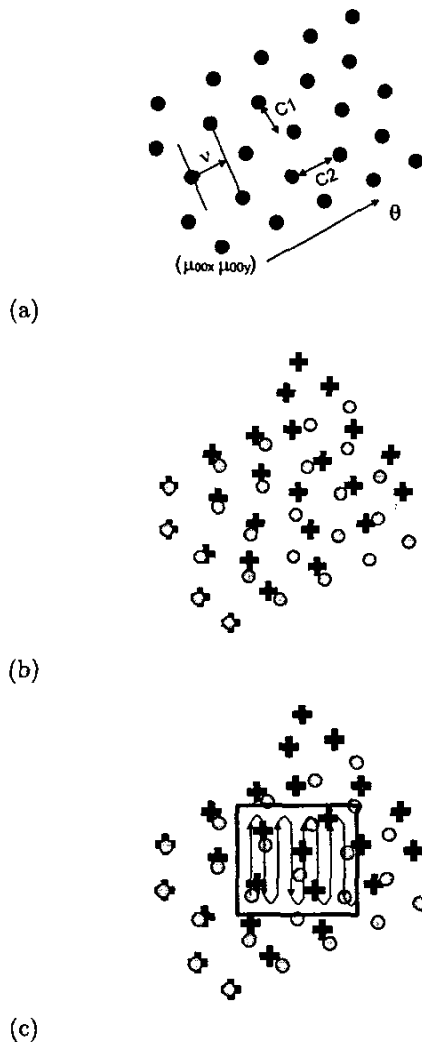


Figure 1: (a) Intended mine locations (circles): six pattern parameters are show on the figure. (b) Actual mine locations (crosses). (c) Detected mine locations in the covered region A : the cover region A is shown as a rectangle.

approach is used to recognize the intended pattern based on the likelihood function. The computation issue related to use of the MLE approach to preform the pattern recognition is described in the section 6. In section 7, we describe the method to construct the probability map based on the recognized pattern. Discussion of the results of the simulation experiments of our method is in Section 8.

2 Relation to Prior Work

The challenging part of our strategy is the pattern recognition. The intended pattern is a finite set of intended mine locations $\mu = \{\mu_i : i = 1, \dots, n\}$ where $\mu_i \in \mathbb{R}^2, i = 1, \dots, n$, which are in some spatial relation with each other. The regular intended pattern is an intended pattern μ , which can be determined by a set of pattern parameters Δ and we denote the regular intended pattern as $\mu(\Delta)$. Regular pattern recognition is to find the intended regular pattern $\mu(\Delta)$ (or equivalent, pattern parameters Δ , because $\mu(\Delta)$ is a function of Δ), which best matches the detected mines in a observation window A . The detected locations are $y_A = \{y_i : i = 1, \dots, y_k\}$, where $y_i \in A, i = 1, \dots, k$ and A is the observation window.

The regular pattern recognition is a difficult task because of the random difference between the intended mine locations (pattern) (Figure 1(a) as an example) and the detected mine locations (Figure 1(c) as an example). Generally, we can decompose the random difference into two sources: errors in the mine laying process and errors in the mine detecting process. The errors in the mine laying process makes the actual laid locations of the mines $x = \{x_i \in \mathbb{R}^2 : i = 1, \dots, n\}$ different than the intended locations $\mu(\Delta)$. Furthermore, because of the false negative errors in the mine detecting process, not all actual mines in the searched area A are detected. The detected mine positions y_A are a subset of the actual mine positions located in A . So, there is no position error in detection.

In previous work [9], we modelled the random errors in both the mine laying process and the mine-detecting process. The mine laying process model $p(x|\mu(\Delta))$ specifies the probability density function of actual mine locations x given the intended locations $\mu(\Delta)$.¹ The model assumes that mines are intended to be placed at regularly spaced intervals along a row. However, during the mine-laying process, the actual mines are placed somewhere around the intended locations and are distributed mutually

¹The interpretation of $p(x|\mu(\Delta))$ is that $p(x|\mu(\Delta))dx_1 \dots dx_n$ is the probability that there are n actual mines and every intended mine $\mu_i(\Delta)$ is actually located in an infinitesimal ball $B(x_i)$ with volume dx_i for $i = 1, \dots, n$.

independently according to a distribution with a density function $p_X(x_i|\mu_i(\Delta))$ for each mine. Therefore, $p(\mathbf{x}|\mu(\Delta)) = \prod_{i=1}^n p_X(x_i|\mu_i(\Delta))$.

The mine detection model specifies the probability law of detected mine locations \mathbf{y}_A given the actual locations \mathbf{x} . The model assumes that the mine detector has a constant false negative error rate. Therefore, the detected mine position in A , \mathbf{y}_A is a subset of $\{x_i : x_i \in A\}$. Based on the mine laying process model $p(\mathbf{x}|\mu(\Delta))$ and the mine detection model, we can specify the probability density function of the random vector \mathbf{y}_A given Δ , $p(\mathbf{y}_A|\mu(\Delta))$. Given data \mathbf{y}_A , the likelihood function $L(\Delta|\mathbf{y}_A)$, a function of Δ , is defined as

$$L(\Delta|\mathbf{y}_A) \equiv p(\mathbf{y}_A|\mu(\Delta)). \quad (1)$$

This provides a matching function between observed data \mathbf{y}_A and the intended pattern $\mu(\Delta)$; a higher value of the likelihood function makes a better match between the intended pattern and the observed data. Then, the pattern recognition is based on the maximization of the likelihood function $L(\Delta|\mathbf{y}_A)$.

3 Contribution

In this paper, we consider a more general error structure in the mine laying process model, which enables us to recognize the pattern when there is a more complicated mine laying process error structure. We begin our effort by examining the mine laying process more carefully. Usually, mines are laid by a mine layer and the laying process involves two actions: layer movement (m) and mine laying (l). The whole mine laying process begins with an initial mine laying followed by a repeated sequence of layer movements and mine laying, that is $(l_0, m_1, l_1, \dots, m_n, l_n)$.

Let $\eta_i \in R^2$ be the mine layer position after m_i , the i th movement action and let x_i be the actual position of the mine in the i th laying action l_i given that the mine layer is at position η_i . The laying process intends to follow the intended pattern, that is, if there is no error in either m_i and l_i then $x_i = \eta_i = \mu_i(\Delta)$ for $i = 1, \dots, n$. But, usually, η_i will be different from $\mu_i(\Delta)$. Such a difference could be specified by a mine layer movement model $p(\eta|\mu(\Delta))$. Note that η_i s are mutually dependent.

Similarly, we expect x_i to be different from η_i . A mine laying model $p(\mathbf{x}|\eta)$ specifies these differences. Therefore, a general mine laying process model should be a two-level hierarchical model: a layer movement model and a mine laying model. Our previous work [9] is a special case of the general model discussed above; the previous model assumes that $\mu_i(\Delta) = \eta_i \neq x_i$, so it eliminates the layer movement model.

In Section 4, we provide the detailed description of a specific two-level hierarchical mine laying process model. The new model allows us to capture the systematic increase of the difference between x_i and $\mu_i(\Delta)$, and increased variability in that difference accumulated along the mine laying process.

4 Hierarchical Probability Model

4.1 Intended Grid Pattern

Before describing the probability models, let's describe the specific regular pattern we used. Following our previous research [9], we continue to assume that the intended pattern is a column-shifted grid pattern as shown in Figure 2. That is, mine laying process begins with $\mu_{0,0}$. $\mu_{0,0} = (\mu_{0,0}^{(x)}, \mu_{0,0}^{(y)})$ is the intended position of the $(0,0)$ mine with respect to a Cartesian robot coordinate frame. We use (i, j) to index the mine at the row i and column j . $(0,0)$ mine is the row 0 and column 0 mine. Then, the mine layer continues to lay mines at positions $\mu_{0,1}, \mu_{0,2}, \dots$ along θ direction with equal distance C_1 apart in row 0. The mines in row 1 begin with $\mu_{1,0}$, which is ν distance away from $\mu_{0,0}$ in row direction and are laid the same way as we do in row 0. The distance between row 0 and row 1 is C_2 . We continue this pattern to lay the rows 2, 3, Therefore, the intended mine positions $\{\mu_{ij}, (i = 0, 1, \dots; j = 0, 1, \dots)\}$ can be determined by the six parameters, $\Delta = (C_1, C_2, \nu, \theta, \mu_{0,0}^{(x)}, \mu_{0,0}^{(y)})$.

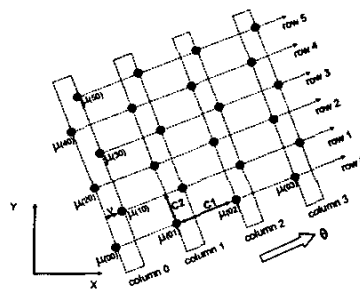


Figure 2: Intended column-shifted grid pattern

4.2 Layer Movement (m_i) Model

In this section, we describe the first level of the hierarchical model: layer movement model $p(\eta|\mu(\Delta))$. (Note that we write Δ as parameters, but later on we see that we need Δ and α as parameters.) Since mines are intended to be laid according to a grid pattern and all rows of mines are laid independently, the

mine layer movement model can be written as

$$\begin{aligned} p(\boldsymbol{\eta}|\boldsymbol{\mu}(\boldsymbol{\Delta})) &= p(\{\eta_{ij}\}|\{\mu_{ij}(\boldsymbol{\Delta})\}) \\ &= \prod_{i=-n}^{n'} p(\{\eta_{ij}, j=0, \dots, m\}|\{\mu_{ij}(\boldsymbol{\Delta}), j=0, \dots, m\}), \end{aligned} \quad (2)$$

where we denote $\{\eta_{ij}\} = \{\eta_{ij}, i = -n, \dots, n'; j = 0, \dots, m\}$ and $\{\mu_{ij}(\boldsymbol{\Delta})\} = \{\mu_{ij}(\boldsymbol{\Delta}), i = 0, \dots, n; j = 0, \dots, m\}$.

The key for the layer movement model is to describe $p(\{\eta_{ij}, j=0, \dots, m\} | \{\mu_{i,j}(\boldsymbol{\Delta}), j=0, \dots, m\})$, the model for mine layer positions in laying every row. Since the model for every row is the same, we delete index i in the notation of the rest of this section for simplicity. $\{\eta_j\} \equiv \{\eta_{ij}, j=0, \dots, m\}$ and $\{\mu_j(\boldsymbol{\Delta})\} \equiv \{\mu_{i,j}(\boldsymbol{\Delta}), j=0, \dots, m\}$, where there are $1+n+n'$ rows and $1+m$ columns.

It is natural to incorporate the sequential characteristic of mine layer movements into our model, therefore, we rewrite our density function sequentially as

$$p(\{\eta_j\}|\{\mu_j(\boldsymbol{\Delta})\}) = \prod_{j=0}^m p(\eta_j|\eta_{j-1}, \dots, \eta_0, \{\mu_j(\boldsymbol{\Delta})\}). \quad (3)$$

Note, when $j = 0$, we denote $p(\eta_j|\eta_{j-1}, \dots, \eta_0, \{\mu_j(\boldsymbol{\Delta})\}) = p(\eta_0|\{\mu_j(\boldsymbol{\Delta})\}) = 1$ if $\eta_0 = \mu_0(\boldsymbol{\Delta})$; 0 otherwise. In the next part, we specify our model for $p(\eta_j|\eta_{j-1}, \dots, \eta_0, \{\mu_j\})$ for $j = 1, \dots, m$.

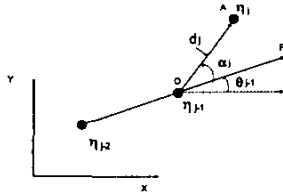


Figure 3: Relationship between the Polar coordinate system and the Cartesian robot coordinate system.

Until now all of the positions are defined according to a Cartesian robot coordinate system. Let's define a polar coordinate system related to the Cartesian coordinate system as shown in Figure 3. The origin O of the polar coordinates is located at η_{j-1} in the Cartesian coordinates; and the initial ray OP is θ_{j-1} degrees away from the positive x -axis of the Cartesian coordinates, where θ_{j-1} is the angle between direction from η_{j-2} to η_{j-1} and the direction of the positive x -axis direction. Therefore,

$$\theta_{j-1} = \arctan \frac{\eta_{j-1}^{(y)} - \eta_{j-2}^{(y)}}{\eta_{j-1}^{(x)} - \eta_{j-2}^{(x)}},$$

when $j > 1$ and also we define $\theta_0 = \theta$ when $j = 1$. The polar coordinates (d_j, α_j) and the cartesian coordinates $(\eta_j^{(x)}, \eta_j^{(y)})$ of the same point η_j have one-to-one relationship with each other.

Let d_j and α_j be the distance and angle of η_j in the polar coordinates. Given $\eta_{j-1}, \dots, \eta_0$, we model d_j and α_j as two independent normal random variables,

$$d_j \sim Normal(C_1, \sigma_d^2), \quad \alpha_j \sim Normal(\alpha, \sigma_\alpha^2), \quad (4)$$

where C_1 is the intended moving distance, σ_d^2 is the variance in moving distance, α represents the systematic (mean) directional divergence and σ_α^2 represents the variability of the directional divergence. The joint distribution of (d_j, α_j) conditional on $\eta_{j-1}, \dots, \eta_0$ and $\{\mu_j\}$ is a bivariate normal distribution in the Polar coordinates. The probability $p(\{\eta_j\}|\{\mu_j(\boldsymbol{\Delta})\})$ now transfers to probability $p(\{\eta_j\}|\{\mu_j(\boldsymbol{\Delta}), \alpha\})$.

Usually, σ_α and σ_d are small. Then we can approximate the original distribution (4) as a bivariate normal distribution in terms of the Cartesian coordinates using the transformation relationship between $(\eta_j^{(x)}, \eta_j^{(y)})$ and (d_j, α_j) . The conditional density of η_j (i.e. the j th term in the product of Equation 3) in the Cartesian coordinates can be expressed as

$$\begin{aligned} p((\eta_j^{(x)}, \eta_j^{(y)})|\eta_{j-1}, \dots, \eta_0, \{\mu_j(\boldsymbol{\Delta}), \alpha\}) \\ \approx N_{\eta_j}(A_{j1}\eta_{j-1} + A_{j2}\eta_{j-2} + u_j, \Sigma_j). \end{aligned} \quad (5)$$

where N_{η_j} represents the bivariate normal density function that describe η_j ; the mean is $A_{j1}\eta_{j-1} + A_{j2}\eta_{j-2} + u_j$ and the variance is Σ_j . A_{j1}, A_{j2}, u_j and Σ_j are functions of $\boldsymbol{\Delta}, \alpha, \sigma_d$ and σ_α . Note that lots of details were omitted to derive at A_{j1}, A_{j2} .

Based on (3) and (5), the joint distribution of $\{\eta_j\} = \eta_0, \dots, \eta_m$ conditional on $\{\mu_j(\boldsymbol{\Delta})\}$ has a density function

$$\begin{aligned} p(\{\eta_j\}|\{\mu_j(\boldsymbol{\Delta}), \alpha\}) \\ = \prod_{j=0}^m N_{\eta_j}(A_{j1}\eta_{j-1} + A_{j2}\eta_{j-2} + u_j, \Sigma_j), \end{aligned} \quad (6)$$

When $j = 0$, we define $N_{\eta_j}(A_{j1}\eta_{j-1} + A_{j2}\eta_{j-2} + u_j, \Sigma_j) = 1$ if $\eta_0 = \mu_0(\boldsymbol{\Delta})$; 0 otherwise.

From (6), we prove that the joint distribution of $\{\eta_j\}$ is a multivariate normal distribution. Because of space restrictions, we do not show the proof. Now, lets return index i back and denote the joint distribution of $\boldsymbol{\eta}_i \equiv \{\eta_{i,j}, j = 0, \dots, m\}$ as

$$p(\{\boldsymbol{\eta}_i\}|\boldsymbol{\mu}(\boldsymbol{\Delta}), \alpha) = N_{\boldsymbol{\eta}_i}(\tilde{\boldsymbol{\eta}}_i, \boldsymbol{\Sigma}_i), \quad (7)$$

where $\tilde{\boldsymbol{\eta}}_i$ and $\boldsymbol{\Sigma}_i$ are functions of $\boldsymbol{\Delta}, \alpha, \sigma_d$ and σ_α .

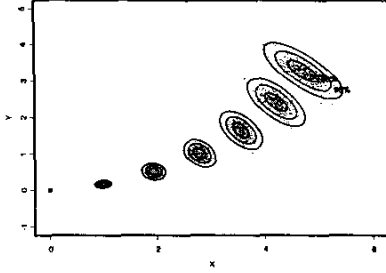


Figure 4: An example of simulated layer positions based the approximated layer movement model. Model parameters: $\eta_0 = (0, 0)$, $d = 1$, $\sigma_d = 0.05$, $\theta = 0^\circ$, $\alpha = 10^\circ$, and $\sigma_\alpha = 2^\circ$.

Figure 4 shows the simulated mine layer positions in multiple steps based on (7). Small grey dots represent the simulated mine layer positions. This illustrates the effect of the accumulated distancing errors and accumulated and systematic directional errors in the multiple steps of the mine layer movement. A mine-layer is originally at position η_0 with direction θ and intends to move at C_1 distance along the θ direction. Because of the systematic directional error α , the laying direction diverges from the original direction in every step. We see that the variability of the layer position increases after every step of moving. The large ellipses are the contour plots of the marginal probability distribution of the layer position calculated from the model (7).

4.3 Mine Laying Model l_i

Now, let's describe the second level of the hierarchical mine laying process model: mine laying model $p(\mathbf{x}|\boldsymbol{\eta})$. We assume that mines are laid independently of each other given the mine layer positions; therefore, the mine laying model can be written as

$$p(\mathbf{x}|\boldsymbol{\eta}) = p(\{x_{i,j}\}|\{\eta_{i,j}\}) = \prod_{i=0}^n \prod_{j=0}^m p(x_{i,j}|\eta_{i,j}), \quad (8)$$

where $x_{i,j}$ represents the actual mine laying position and $\eta_{i,j}$ as the position of the mine-layer. As in our original model, we choose the normal density to specify the conditional probability density of $x_{i,j}$ given $\eta_{i,j}$:

$$p(x_{i,j}|\eta_{i,j}) = N_{x_{i,j}}(\eta_{i,j}, \Sigma), \quad (9)$$

where $\Sigma = \text{diag}\{\sigma^2, \sigma^2\}$.

4.4 Mine Detecting Model

The assumptions of the mine detecting model are the same as those used in the previous model. A simple

model is used to model the false negative error of the mine detector. That is, for every mine located at $x_{i,j}$ in the minefield,

$$\alpha_{i,j} = \begin{cases} 1, & \text{if detected} & \text{with probability } p_d; \\ 0, & \text{if undetected} & \text{with probability } 1 - p_d, \end{cases}$$

which assumes that every mine has the same probability to be detected no matter its location in the minefield and the detection is independent with each other. Therefore, the detected mine positions in A is a subset of the mines actually located in A , that is $\mathbf{y}_A = \{x_{i,j} : x_{i,j} \in A\}$. Now we have our probability model, from next section, we are going to describe how to decode the pattern parameters based on the probability model.

5 Likelihood Function

In this section, we derive the likelihood function, which we use to decode the pattern parameters in section 6. The parameter vector to characterize the curved grid pattern is now $\Delta = (C_1, C_2, \nu, \theta, \mu_{0,0}^{(x)}, \mu_{0,0}^{(y)})$ and α . What we observe in the covered region A are detected mines at positions $\mathbf{y}_A = (y_1, \dots, y_k)$, where $\mathbf{y}_i \in A$, $i = 1, \dots, k$. Let $p(\mathbf{y}_A|\Delta, \alpha)$ be the joint probability density of the detected mines \mathbf{y}_A . Given that \mathbf{y}_A is observed, the likelihood function of Δ, α is defined as

$$\begin{aligned} L(\Delta, \alpha|\mathbf{y}_A) &= p(\mathbf{y}_A|\Delta, \alpha) \\ &= \int \cdots \int_{\{\eta_{i,j}\}} p(\mathbf{y}_A|\{\eta_{i,j}\}) p(\{\eta_{i,j}\}|\{\mu_{i,j}(\Delta)\}, \alpha) d\{\eta_{i,j}\} \end{aligned} \quad (10)$$

We discuss how to approximate $p(\mathbf{y}_A|\{\eta_{i,j}\})$ in section 5.1. The evaluation of the full likelihood function (10) is discussed in section (5.2). σ_d , σ_α and σ are also parameters in the density function $p(\mathbf{y}_A|\Delta, \alpha)$. Since we assume that they are known and small, we do not list them as the parameters in the likelihood function.

5.1 Approximate $p(\mathbf{y}_A|\{\eta_{i,j}\})$

Since the assumptions of the mine detecting model in this paper are the same as those of the mine laying process model and the mine detecting model in [9], the derivation of $p(\mathbf{y}_A|\{\eta_{i,j}\})$ is similar as the derivation of $p(\mathbf{y}_A|\boldsymbol{\mu}(\Delta))$ in (1). Here, we outline the result of evaluating $p(\mathbf{y}_A|\{\eta_{i,j}\})$. See [9] for some more detailed discussion.

Evaluation of the exact formula of $p(\mathbf{y}_A|\boldsymbol{\mu}(\Delta))$ and $p(\mathbf{y}_A|\{\eta_{i,j}\})$ are generally intractable. Here we provide the approximated formula when σ , σ_d and σ_α are small, which holds in our application. Based on the small variance assumption, we could almost

surely label with the (i, j) index all detected mine located at y_s ($y_s \in \mathbf{y}_A$, and $i = 1, \dots, k$) given Δ, α . Based on this index information, we can define a one-to-one mapping ϕ , where

$$\phi : \{1, \dots, k\} \rightarrow \{(i, j) : \eta_{i,j} \in W\},$$

such that the index for the y_s is $(i, j) = \phi(s)$. When $\phi^{-1}((i, j)) = \emptyset$, it means that (i, j) mine is not detected. When $\phi^{-1}((i, j)) \neq \emptyset$, the (i, j) mine is detected and the detected (actual) location is $x_{i,j} = y_{\phi^{-1}((i, j))}$.² Therefore, the probability density that the (i, j) mine is observed and its actual location is $x_{i,j}$ is

$$p_{\text{det}}(x_{i,j}|\eta_{i,j}) = p_d p(x_{i,j}|\eta_{i,j}), \quad (11)$$

where $p(x_{i,j}|\eta_{i,j})$ is specified in (9).

The probability that (i, j) mine is not observed in A is

$$\begin{aligned} & \mathcal{P}_{\text{ud}}(\phi^{-1}((i, j)) = \emptyset|\eta_{i,j}) \\ &= \int_{\mathbb{R}^2 \setminus A} p_d p(x_{i,j}|\eta_{i,j}) dx_{i,j} + (1 - p_d), \end{aligned} \quad (12)$$

or we can rewrite (12) in another form as

$$\left[\int_{\mathbb{R}^2 \setminus A} + \frac{1-p_d}{p_d} \int_{\mathbb{R}^2} \right] p_d p(x_{i,j}|\eta_{i,j}) dx_{i,j} \quad (13)$$

For notational simplicity, lets denote

$$p_\phi((i, j), \eta_{i,j}) \equiv \begin{cases} p_{\text{det}}(x_{i,j}|\eta_{i,j}), & \text{if } \phi^{-1}((i, j)) \neq \emptyset; \\ \mathcal{P}_{\text{ud}}(\emptyset|\eta_{i,j}), & \text{if } \phi^{-1}((i, j)) = \emptyset, \end{cases} \quad (14)$$

where $x_{i,j} = y_{\phi^{-1}((i, j))}$ when $\phi^{-1}((i, j)) \neq \emptyset$.

Then, we have the following result:

$$p(\mathbf{y}_A|\{\eta_{i,j}\}) \approx \prod_{i=-n}^{n'} \prod_{j=0}^m p_\phi((i, j), \eta_{i,j}) \quad (15)$$

5.2 Evaluate $L(\Delta, \alpha|\mathbf{y}_A)$

Based on $p(\mathbf{y}_A|\{\eta_{i,j}\})$ in equation (15) and $p(\{\eta_{i,j}\}|\{\mu_{i,j}(\Delta)\})$ in equation (7), the likelihood function $L(\Delta, \alpha|\mathbf{y}_A)$ (10) can be be rewritten as:

$$L(\Delta, \alpha|\mathbf{y}_A) = \prod_{i=-n}^{n'} \int \dots \int_{\{\eta_{i,j}\}} \Omega d\{\eta_{i,j}, j = 0, \dots, m\}, \quad (16)$$

where, $\Omega = \prod_{j=0}^m p_\phi((i, j), \eta_{i,j}) N_{\eta_i}(\tilde{\eta}_i, \Sigma_i)$. Then, by switching the integral between $\int_{\{\eta_{i,j}\}}$ and

²Note, we consider detector error, but if the detector detects the mine, then it actually detects its location.

$\left[\int_{\mathbb{R}^2 \setminus A} + \frac{1-p_d}{p_d} \int_{\mathbb{R}^2} \right]$, which is used in evaluating $p_\phi((i, j), \eta_{i,j})$ when $\phi^{-1}((i, j)) = \emptyset$, (16) becomes

$$\begin{aligned} & \prod_{\{(i, j) : \phi^{-1}((i, j)) = \emptyset\}} \left[\int_{\mathbb{R}^2 \setminus A} + \frac{1-p_d}{p_d} \int_{\mathbb{R}^2} \right] d\{x_{i,j}\} \\ & \prod_{i=-n}^{n'} \int \dots \int_{\{\eta_{i,j}\}} \Omega' d\{\eta_{i,j}, j = 0, \dots, m\}, \end{aligned} \quad (17)$$

where, $\Omega' = \prod_{j=0}^m p_d p(x_{i,j}|\eta_{i,j}) N_{\eta_i}(\tilde{\eta}_i, \Sigma_i)$. Based on the model (9), $\prod_{j=0}^m p(x_{i,j}|\eta_{i,j})$ can be written in the form of a multivariate normal density of $\mathbf{x}_i = \{x_{i,0}, \dots, x_{i,m}\}$ given $\eta_i = \{\eta_{i,0}, \dots, \eta_{i,m}\}$ as $N_{\mathbf{x}_i}(\eta_i, \Sigma)$, where $\Sigma = \text{diag}\{\Sigma, \dots, \Sigma\}$. Then, we have

$$\begin{aligned} & \prod_{i=0}^m p_d p(x_{i,j}|\eta_{i,j}) N_{\eta_i}(\tilde{\eta}_i, \Sigma_i) \\ &= N_{\mathbf{x}_i}(\eta_i, \Sigma) N_{\eta_i}(\tilde{\eta}_i, \Sigma_i) \end{aligned}$$

Therefore, (17) becomes

$$\begin{aligned} L &= \prod_{\{(i, j) : \phi^{-1}((i, j)) = \emptyset\}} \left[\int_{\mathbb{R}^2 \setminus A} + \frac{1-p_d}{p_d} \int_{\mathbb{R}^2} \right] d\{x_{i,j}\} \\ & \prod_{i=-n}^{n'} N_{\mathbf{x}_i}(\tilde{\eta}_i, \Sigma + \Sigma_i), \end{aligned} \quad (18)$$

which can be evaluated numerically by some further approximation. Because of space limitations, we will not describe the details here. Therefore, we approximate the likelihood function, which can be evaluated relatively easily.

6 Efficient Maximum Likelihood Estimation

The parameters Δ and α are estimated by maximizing the likelihood function $L(\Delta, \alpha|\mathbf{y}_A)$, as shown in equation (10). That is, the Maximum Likelihood Estimator (MLE)

$$(\Delta, \alpha)^m = \text{argmax}_{\Delta, \alpha} L(\Delta, \alpha|\mathbf{y}_A) \quad (19)$$

Evaluating $(\Delta, \alpha)^m$ is computational challenging. There are two major challenges. First, the integration of the likelihood function (10) does not have closed form. To make matters worse, $L(\Delta, \alpha|\mathbf{y}_A)$ has many local maxima; and, the likelihood function around the local maximum could be very peaked, but, its value could drop to zero very quickly. All of this makes finding the parameters that globally maximize the likelihood function difficult.

There exists a general and well-understood technique for hill-climbing in likelihood space: the *EM algorithm* [4], which in the context of Hidden Markov

Models is often referred to as *Baum-Welch* or *alpha-beta* algorithm [7]. EM is a hill-climbing routine in likelihood space which alternates two steps, an *expectation step* (E-step) and a *maximization step* (M-step). Iterative application of both steps leads to a refinement of both the pattern parameters and layer motions, therefore avoids evaluating the integral in the likelihood function. Existing HMM algorithms assume the state space of the environment (pattern parameters Δ, α) and its observation space (mine layer positions) $\{\eta_{i,j}\}$ are discrete, which is not the case in our application. Some researchers have developed algorithms that support continuous state and actions spaces [6] [8]. However computational complexity prevents on-line implementation of the algorithm on the available resources of a mobile robot. Moreover, the algorithm converges to a local maximum in likelihood space, no global maximum can be guaranteed.

In our research, we approximate the likelihood function $L(\Delta, \alpha | \mathbf{y}_A)$ (10) using a multivariate normal distribution approximation. The approximate likelihood (18) dramatically decreases the computational complexity in likelihood function evaluation because of the nice properties of the normal distribution. This is way we approximate the likelihood function in section 5.

A global maximum is guaranteed by a mode directing algorithm. The mode directing algorithm identifies all possible local maximum areas and directs the optimization routing to search each local maximum. In the next part, we discuss the details of the mode directing algorithm.

6.1 Mode Directing Algorithm

It is practically impossible to apply any general optimization algorithm to maximize the approximate likelihood function (18) to get $(\Delta, \alpha)^m$. The algorithm will be very inefficient because of the specialty of the likelihood function. First, the likelihood function has many local maxima. Second, the likelihood function could peak very quickly around the local maxima and the function is relatively flat when it is away from maxima. These two characteristics of the likelihood function mean that the general optimization algorithm could easily be trapped in local maxima. The reason that the likelihood function shows these characteristics is explained in our previous paper [9].

The solution to improve the performance of the general optimization algorithm is the mode directing algorithm introduced in [9]. The mode directing algorithm identifies all of the possible local maxima and generates one starting point near every local maximum. Beginning with the local starting point, the

optimization algorithm could reach the local maximum. By directing the general optimization algorithm to all possible local start points, global maximum could be guaranteed.

It is very difficult to develop a mode directing algorithm if the first row of the minefield is not covered in the observation window. In this paper, we provide a partial solution by assuming that the covered region A always includes the first column of the minefield and at least one of the mines in the first column and even number row is detected. It serves the first step to the full solution.

We discretize $\theta \in [0, 2\pi)$. For any $\theta \in [\theta_0, \theta_0 + \Delta\theta]$, let $y_i \in \mathbf{y}_A$ be the found mine location that has the lowest x coordinate value in a new Cartesian coordinate. The new coordinate system has the same origin as the robot coordinate system and the positive x-axis direction is θ degrees away from the positive x-axis of the robot coordinate system. $[\theta_0, \theta_0 + \Delta\theta]$ is short such that for every $\theta \in [\theta_0, \theta_0 + \Delta\theta]$ we will get the same y_i .

Based on our assumptions, we can show that the detected location y_i in at least one of the θ interval is a mine in the first column and even number row. Therefore, we label y_i as the (0, 0) mine. Now, we have the bound for $\mu_{0,0}^{(x)}, \mu_{0,0}^{(y)}, \theta$, and α as follows:

- $\mu_{0,0}^{(x)} \in [y_i^{(x)} - 3\sigma, y_i^{(x)} + 3\sigma]$ and $\mu_{0,0}^{(y)} \in [y_i^{(y)} - 3\sigma, Y_i^{(y)} + 3\sigma]$, where $(y_i^{(x)}, y_i^{(y)})$ is the value of y_i in the robot coordinate system.
- $\theta \in [\theta_0, \theta_0 + \Delta\theta]$, where $\Delta\theta$ is small.
- $\alpha \in [-\alpha_0, \alpha_0]$. α_0 is small, since we assume that the directional error is small.

Since we can identify the (0, 0) mine and bound $(\mu_{0,0}^{(x)}, \mu_{0,0}^{(y)})$ as we do in [9]. By setting $\alpha = 0$, we can apply the mode directing algorithm developed in [9] to find all of the possible local maxima when $\theta \in [\theta_0, \theta_0 + \Delta\theta]$. The possible number of the local maxima is the possible (i, j) label for the second found mine, the found mine nearest to the first mine. The possible (i, j) label and the corresponding parameter starting point can be calculated. Because of space limitations, we will not discuss the details of the calculations.

7 Probability Density Map Building

For the path planing application, the useful summary information is the predicted probability density map of undetected mine locations:

$$p(x | \{\mu_{i,j}(\Delta^m)\}, \alpha^m, \mathbf{y}_A), x \in \mathbb{R}^2. \quad (20)$$

The prediction is based on the detected mine locations in A , y_A and MLEs of the parameters, Δ^m , α^m . The interpretation of the predicted probability density map is that $p(x|\{\mu_{i,j}(\Delta^m)\}, \alpha^m, y_A)dx$ is the probability that an undetected mine is located in an infinitesimal disk centered at x with volume dx .

Then, the predicted density map of mine locations can be used to calculate the predicted expected number of unobserved mines in any area B , $n(B)$, for $B \subset \mathbb{R}^2$; that is

$$E(n(B)|\{\mu_{i,j}(\Delta^m)\}, \alpha^m, y_A) = \int \mathbf{1}_B(x)p(x|\{\mu_{i,j}(\Delta^m)\}, \alpha^m, y_A)dx,$$

where $\mathbf{1}_B(x) = 1$, if $x \in B$, 0 otherwise. Since we have Δ^m, α^m , based on the same argument as in Section 5.1, we could label with (i, j) the actual mine located at x , and all $y_s \in y_A$; therefore, the actual locations that we intend to detect mines x becomes $x_{i',j'}$ and the actual locations we detect mines y_s become $x_{i,j}$ for $s = 1, \dots, k$. Then (20) can be simplified as

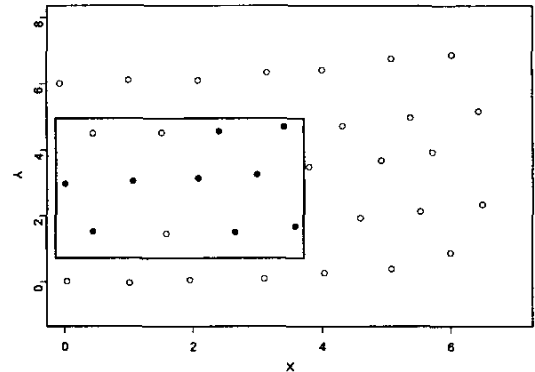
$$p(x_{i',j'}|\{x_{i,j} : \phi^{(-1)}((i,j)) \neq \emptyset, i = i'\}, \{\mu_{i,j}(\Delta^m)\}, \alpha^m).$$

Since the joint distribution of $x_{i',j'}$ and $\{x_{i,j} : \phi^{(-1)}((i,j)) \neq \emptyset, i = i'\}$ is a multivariate normal distribution conditional on $\{\mu_{i,j}(\Delta^m)\}$ and α^m as shown in (18), the distribution of $x_{i',j'}$ conditioning on $\{x_{i,j} : \phi^{(-1)}((i,j)) \neq \emptyset, i = i'\}$ is another normal distribution and can be easily calculated.

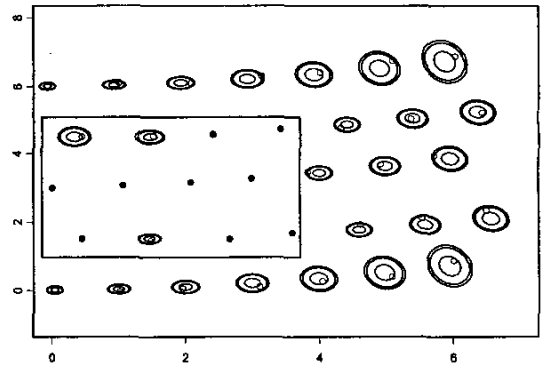
8 Simulation Experiments

The simulation experiments are conducted to exam the performance of the pattern recognition and the map building algorithm. A set of actual mine locations are simulated base on the two-level hierarchical mine laying process model as described in Section 4. Figure 5(a) shows an example of the simulated actual mine locations. All circles represent the actual mines. Then a subset of actual mines inside the rectangle observation region is randomly selected based on the mine detecting model (Section 4.4). The detected mines in the covered region are represented by solid circles. The pattern recognition is conducted using the Maximum Likelihood Estimator method. The mode directing algorithm guarantees that all local maxima are explored, therefore, a global maximum is guaranteed. Furthermore, the multivariate normal approximation makes the evaluation of the likelihood function very efficient. Therefore, the whole algorithm is very efficient and fast. Figure 5(b) shows the contour plot of the predicted probability density map of the undetected mines in the minefield, $p(x|\{\mu_{i,j}(\Delta^m)\}, \alpha^m, y_A)$. The biggest ellipses

surrounding the undetected actual mine locations are the 95% confidence area. There is 95% of chance that a mine is located in one of the biggest ellipses. The ellipses are smaller in rows that some mines are detected. The reason is that the detected mine locations in those rows help decreasing the prediction uncertainty of undetected mine locations. We see that all actual mines are inside the 95% confidence ellipses in this example, which indicates that the pattern recognition algorithm does a good job.



(a)



(b)

Figure 5: (a) Simulated actual and detected mine locations. (b) Contour plot of the predicted probability density map of undetected mine locations

9 Conclusion

This paper extends our original statistical approach to identify the regular pattern of a minefield at the beginning of the searching process. The new approach can capture systematic and accumulated random departure of the actual mine locations from the

grid pattern caused by the inaccuracy of the translational and rotational motion of the mine layer. The extracted pattern parameters can be used to build a probability distribution map of the configuration of the minefield. The map then can be used to guide the search for more mines efficiently.

The simulation evaluations are used to illustrate the performance and efficiency of the probability approach algorithm. The mode partitioning algorithm guarantees that a global maximum is reached efficiently in the optimization algorithm. Because we use the multivariate normal approximation to evaluate the likelihood function, the Maximum Likelihood Estimation evaluation is very efficient. Therefore, online implementation of our pattern search algorithm on a mobile robot is feasible.

Although this paper makes a significant contribution to the design of search strategies when the minefield follows some regular pattern, there remains much more work to be done. Remaining research includes: (i) to extend our methodologies to extract patterns, which belongs to many possible families of the patterns; (ii) to include the detector false positive into our noise model.

References

- [1] Mine/countermine operations. FIELD MANUAL FM 20-32, US Army Engineer School (NEW - FORT LEONARD WOOD), Fort Leonard Wood, MO 65473-5000, 1998.
- [2] E. Acar and H. Choset. Critical point sensing in unknown environments. In *Proc. of IEEE ICRA '00*, San Francisco, CA, 2000.
- [3] H. Choset, E. Acar, A. Rizzi, and J. Luntz. Exact cellular decompositions in terms of critical points of Morse functions. In *Proc. of IEEE ICRA '00*, San Francisco, CA, 2000.
- [4] A. Dempster, A. Laird, and D. Rubin. Maximum likelihood from incomplete data via the em algorithm. *Journal of the Royal Statistical Society, Series B*, 39:1-38, 1977.
- [5] E. Gelenbe and Y. Cao. Autonomous search for mines. *European Journal of Operational Research*, 108:319-333, 1998.
- [6] R.E. Kalman. A new approach to linear filtering and prediction problems. *Trans. ASME, Journal of Basic Engineering*, 82:35-45, 1960.
- [7] L. Rabiner and B. Juang. An introduction to hidden Markov models. In *IEEE ASSP Magazine*, 1986.
- [8] S. Thrun and J. Langford. Monte Carlo hidden Markov models. Technical report, School of Computer Science, Carnegie Mellon University, 1998. CMU-CS-98-179.
- [9] Y. Zhang, M. J. Schervish, E. U. Acar, and H. Choset. Probabilistic methods for robotic landmine search. In *Proc. IROS 2001*, 2001.